Pharm Res (2012) 29:2738–2753
DOI 10.1007/s11095-012-0759-8

RESEARCH PAPER

pH-Induced Precipitation Behavior of Weakly Basic Compounds: Determination of Extent and Duration of Supersaturation Using Potentiometric Titration and Correlation to Solid State Properties

Yi-Ling Hsieh • Grace A. Ilevbare • Bernard Van Eerdenbrugh • Karl J. Box • Manuel Vincente Sanchez-Felix • Lynne S. Taylor

Received: 2 November 2011 / Accepted: 11 April 2012 / Published online: 12 May 2012

ABSTRACT

Purpose To examine the precipitation and supersaturation behavior of ten weak bases in terms of the relationship between pH-concentration-time profiles and the solid state properties of the precipitated material.

Methods Initially the compound was dissolved at low pH, followed by titration with base to induce precipitation. Upon precipitation, small aliquots of acid or base were added to induce slight subsaturation and supersaturation respectively and the resultant pH gradient was determined. The concentration of the unionized species was calculated as a function of time and pH using mass and charge balance equations.

Results Two patterns of behavior were observed in terms of the extent and duration of supersaturation arising following an increase in pH and this behavior could be rationalized based on the crystallization tendency of the compound. For compounds that did not readily crystallize, an amorphous precipitate was formed and a prolonged duration of supersaturation was observed. For compounds that precipitated to crystalline forms, the observed supersaturation was short-lived.

Conclusion This study showed that supersaturation behavior has significant correlation with the solid-state properties of the precipitate and that pH-metric titration methods can be utilized to evaluate the supersaturation behavior.

KEY WORDS amorphous · crystallization · pH-Metric · precipitation · supersaturation

INTRODUCTION

The aqueous solubility of active pharmaceutical ingredients (APIs) is a critical physicochemical property since APIs must first enter the solution phase prior to absorption across a biological membrane. While the solubility of newly discovered APIs in the 1980s was typically above 20 μg/ml, nowadays a solubility of less than 1 μg/ml for new drug candidates is very common (1). Consequently, the poor aqueous solubility of developmental compounds is a well-recognized problem impacting drug delivery. For ionizable compounds, solubility is highly pH-dependent whereby the ionized species nearly always possesses a higher solubility than the unionized species. From a physiological perspective, pH varies in different parts of the gastrointestinal tract with the stomach pH ranging from 1.5 to 3.5 while the duodenum varies between pH 5–7 (2). Weakly basic compounds with pKa values ranging from 5 to 8 can be completely or partially solubilized in the stomach where they will

Y.-L. Hsieh • G. A. Ilevbare • B. Van Eerdenbrugh • L. S. Taylor
Department of Industrial and Physical Pharmacy, College of Pharmacy
Purdue University
West Lafayette, Indiana, USA

B. Van Eerdenbrugh
Laboratory for Pharmacotechnology and Biopharmacy, K.U. Leuven
Leuven, Belgium

K. J. Box
Sirius Analytical
Sussex, UK

M. V. Sanchez-Felix
Eli Lilly and Company
Indianapolis, Indiana, USA

L. S. Taylor (✉)
575 Stadium Mall Dr.
West Lafayette, Indiana 47907, USA
e-mail: lstaylor@purdue.edu

form ionized species; however, as the pH increases in the lower regions of the GI tract, weak bases are prone to precipitate because of the lower solubility of the unionized species, as illustrated schematically in Fig. 1a. According to classical nucleation theory and phenomenological observation (3), if a solution is sufficiently supersaturated with respect to the equilibrium solubility of the crystalline form, spontaneous nucleation will occur, and will be followed by crystal growth. Supersaturation is a non-equilibrium condition whereby the solution concentration (or more rigorously, chemical potential) exceeds the equilibrium solubility (chemical potential of the saturated solution). Equilibrium is reached by phase separation to a crystalline solid. The

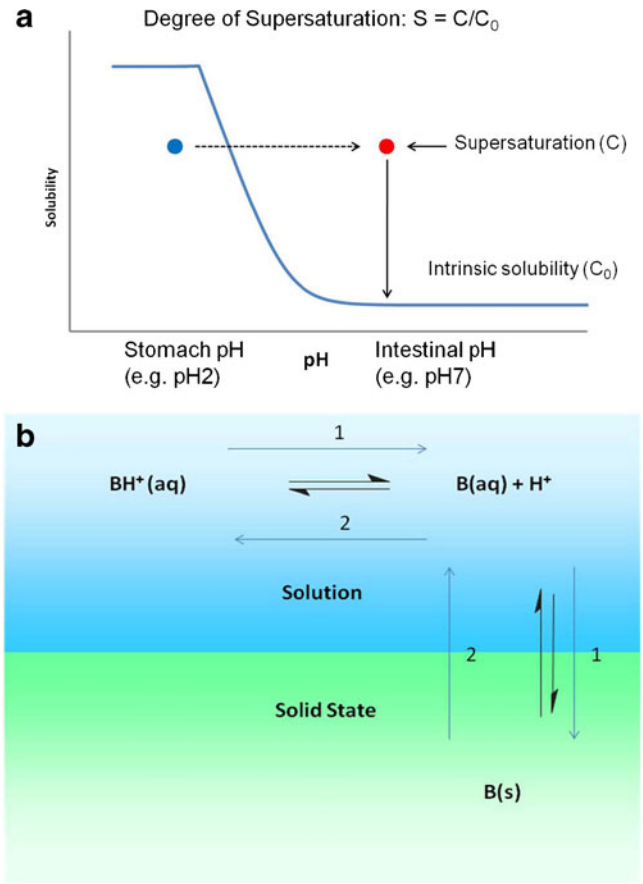

Fig. 1 (**a**) Schematic of precipitation of a weakly basic compound in GI tract. Initially, the compound is completely solublized at low pH. In higher pH regions of the GI tract, formation of the less soluble unionized species increases and hence solubility decreases. Consequently the initially completely solublized drug in stomach becomes supersaturated upon entering the intestinal region. (**b**) Schematic of drug precipitation showing release or consumption of protons in solution. Direction 1: free base precipitation shifts the aqueous equilibrium to replace the B that is lost from solution. Consequently protons are released into solution and the pH goes down. Direction 2: free base dissolution shifts the aqueous equilibrium to produce more BH^+ and keep the concentration of B (aq) near the solubility concentration. Consequently protons are consumed from solution and the pH goes up. In other words, adding a base into solution makes the pH go up, removing a base from solution (through precipitation) makes the pH go down.

impact of pH changes in the GI tract on dissolution, supersaturation and drug absorption has been studied previously (4,5). It is widely accepted that a prolonged duration of supersaturation can significantly improve bioavailability, in particular for poorly soluble compounds for which absorption is limited due to the low *in vivo* GI concentrations. Hence various formulation approaches have been employed that result in the generation of a supersaturated solution (4–7), many of which employ polymers to retard precipitation in the GI tract (8,9). However, it has been acknowledged that there is a fundamental lack of understanding of precipitation phenomena (10).

Obtaining information about the intrinsic solubility of the unionized crystalline compound, as well as the concentration at which precipitation occurs (sometimes termed the kinetic solubility) is essential for assessing the extent and duration of supersaturation. For ionizable compounds, a potentiometric method, termed the chasing equilibrium method (CheqSol), has been developed to rapidly measure kinetic and equilibrium solubilities (11). Equilibrium or intrinsic solubility is the solution concentration where the crystalline solid (most thermodynamically stable phase) and solution phase are at equilibrium. Kinetic solubility has been defined as the concentration where precipitation first starts to appear during the process of inducing precipitation (11). In the chasing equilibrium method of solubility determination, the compound is first dissolved in aqueous solution at a pH where the compound is completely ionized and then the solubility is reduced by increasing the neutral species concentration through a pH shift. Thus for a base, after complete solubilization in a low pH environment, basic titrant is added to the solution to increase pH and produce the unionized species. When a certain extent of supersaturation is produced through generation of the unionized form, precipitation commences. The pH where precipitation first occurs, which is detected by an *in situ* ultraviolet/visible (UV/Vis) probe, is used to determine the kinetic solubility. After the initial detection of precipitation, additional titrant is added to induce more precipitation and then the pH is monitored to allow the scientist to follow the process of drug precipitation from supersaturated solution. A consequence of a basic drug precipitating and crystallizing from solution is the generation of a negative pH gradient with respect to time (dpH/dt) which develops because of the release of protons into solution (see Fig. 1b). As the system moves towards attaining equilibrium, the pH is then changed in one direction or the other by adding small amounts of acidic or basic titrant. Following these small changes in pH, the system becomes either subsaturated (addition of acidic titrant) or supersaturated (addition of basic titrant) leading to dissolution or additional precipitation respectively. The pH gradients and rate of pH change caused by release of protons into solution (precipitation of

the basic solute, decrease in pH) or consumption of protons (dissolution of basic solute, increase in pH) can be used to indicate the extent of saturation in solution. Thus for a basic compound, a negative pH-gradient indicates supersaturation while a positive pH gradient results from subsaturation and consequent dissolution. By alternatively adding small aliquots of acid and base titrant ("pH swing" process), and monitoring the pH gradient, the equilibrium solubility can be estimated from the point at which the pH gradient becomes zero, *i.e.* where no net dissolution or precipitation occurs. The solubility of the neutral species at the zero gradient point is calculated from a series of mass and charge balance equations (12). Using this method, two types of behavior have been observed: Type 1 where the concentration of the neutral species at the precipitation point (kinetic solubility) is considerably higher than the measured equilibrium solubility, *i.e.* supersaturation is present prior to precipitation. Type 1 compounds "chase" equilibrium when the pH is cycled following the initial precipitation of the neutral form, undergoing small amounts of dissolution and precipitation in response to pH changes, and hence have been termed "chasers". In contrast, type 2 compounds precipitate rapidly and do not appear to supersaturate prior to precipitation and instead of observing the development of pH gradients during the pH cycling portion of the experiment, these compounds instantaneously respond to the change in pH; hence they have been called "non-chasers" (11). It is clearly of interest to develop an improved understanding of the origin of these differences in behavior. The timeframe over which compounds respond to changes in pH by dissolving or precipitating is of obvious physiological relevance. Intuitively, the ability to supersaturate should also be related to the crystallization tendency of the compound in the solid state, which has been the subject of recent investigations in our lab (13,14). Hence the goal of the current study was to investigate the precipitation behavior of a number of compounds in terms of the extent and duration of the supersaturation generated by pH change, and to relate the solution profiles to the solid state properties of the resultant precipitated material. A further goal was to discuss the potential pharmaceutical relevance of these observed differences in behavior.

MATERIALS AND METHODS

Materials

Bifonazole and pyrimethamine were purchased from Spectrum Chemical (Gardena, CA). Dipyridamole, droperidol, clotrimazole and papaverine HCl were purchased from Sigma-Aldrich (St. Louis, MO). Papaverine free base was prepared from the HCl salt by a method described in the publication by Miyajima *et al.* (15). Carvedilol and loratadine were purchased from Attix (Toronto, Ontario, Canada). Ketoconazole and clozapine were purchased from Hawkins, Inc (Minneapolis, MO) and Euroasia (Mumbai, India) respectively. Basic titrant was prepared by diluting carbon dioxide free potassium hydroxide concentrate (Mallinckrodt Baker Inc, Phillipsburgh, NJ) to 0.5 N. The ionic strength of water was adjusted to 0.15 M with potassium chloride (Mallinckrodt Baker Inc, Phillipsburgh, NJ). 0.5 N hydrochloric acid standard solution purchased from Sigma-Aldrich was used as acid titrant.

pKa Titration

A Sirius GLpKa titrator equipped with a pH electrode and a Sirius D-PAS unit with a 1 cm path length UV dip probe (Hellma, Southend-on-Sea, Essex, UK) were used to perform pKa titrations. The instrument was controlled by Refinement Pro software (Sirius Analytical instruments Ltd., Forest Row, East Sussex, UK). Calibration of the pH electrode was done in the pH range of 1.8-12.2 by software-controlled addition of the aforementioned acid and basic titrants. The temperature was maintained at 37°C by a VWR heating circulating bath 1160 S (VWR International, Radnor, PA). The GLpKa unit was equipped with a nitrogen purge over the titrants and solutions to minimize dissolution of carbon dioxide.

pKa values for seven of the compounds (clozapine, dipyridamole, droperidol, ketoconazole, loratadine, papaverine and pyrimethamine) were determined from pH-dependent multi-wavelength UV spectra collected by the D-PAS system. In each experiment, 15.00 mL of an aqueous solution of sample (initial concentration between 19 and 100 μM) was pre-acidified to pH 1.8-2.0 with 0.5 M HCl, and then titrated with 0.5 M KOH to high pH. The titrations were carried out at constant ionic strength (0.15 M KCl) and temperature (t= 37.0±0.5°C), and under a nitrogen atmosphere. A minimum of five parallel measurements were carried out and the pK_a values of samples were calculated by RefinementPro™ software (Sirius Analytical Instruments Ltd., Forest Row, UK). Methodologies used by the software have been described in an earlier publication (16).

The cosolvent dissociation constants (p$_s K_a$ values) of two of the most insoluble compounds (bifonazole and clotrimazole) were determined in various methanol–water mixtures between 8 and 52 wt% using pH-dependent multi-wavelength UV spectra collected by the D-PAS system. The same titration protocol was performed as described above. Each sample was measured in at least five different methanol–water mixtures at concentrations ranging from 26 to 200 μM. The measured p$_s K_a$ values in methanol–water were extrapolated to aqueous conditions according to the Yasuda-Shedlovsky procedure, which is the most widely used method among cosolvent techniques (17,18).

The cosolvent dissociation constants (p$_s K_a$ values) of carvedilol were determined in various methanol–water

mixtures between 8 and 39 wt% using the pH-metric approach (as the ionizable group was remote from a UV chromophore and the multi-wavelength UV spectra were independent of pH). The same titration protocol was performed as described above and carvedilol was measured at least in eight different methanol–water mixtures at concentrations ranging from 0.3 to 0.8 mM. The titration data was subjected to a series of mass and charge balance equations to determine the p_sK_a values in methanol–water and these were extrapolated to aqueous conditions using the Yasuda-Shedlovsky procedure. Methodologies used by the software have been described in an earlier publication (19).

pH Solubility Titration

The Sirius GLpKa titrator described above was used for these experiments. pH titrations were performed using the Cheqsol method described above, for which further details can be found in earlier publications (11,12).

Solid State Characterization

The slurries with precipitates obtained from pH titration were first evaluated with an Eclipse E600 POL polarized light microscope equipped with DS-Fi1 camera (Nikon Corporation, Tokyo, Japan) for the presence or absence of birefringence. Separation of supernatant and precipitates were achieved by ultracentrifugation at 40,000 RPM (equivalent to 274,356 × g) in an Optima L-100 XP ultracentrifuge equipped with Swinging-Bucket Rotor SW 41 Ti (Beckman Coulter, Inc., Brea, CA). The precipitates were dried in vacuum for 24 h. A TA Q2000 differential scanning calorimeter (DSC) with a refrigerated cooling accessory (TA Instruments, New Castle, DE) was used to detect the presence of glass transition, crystallization and melting events in the precipitated solids. For the precipitate, the solids were first equilibrated at −50°C and then heated to 10°C above the melting point at a heating rate of 5°C/min. The methods described by Baird *et al.* (13) and Van Eerdenbrugh *et al.* (14) were used to determine the crystallization tendency classification of each compound, using the original material as supplied for these measurements (Table I). The melting temperature and enthalpy of fusion were recorded from experiments on the original material. Pyrimethamine could not be classified using these two methods due to its tendency to degrade upon melting and low solubility in the selected organic solvents (dichloromethane and methanol) which is insufficient to enable spin-coating.

The moisture sorption profiles of amorphous carvedilol, ketoconzole, clotrimazole, loratadine and clozapine were determined at 37°C using a TA Q5000 dynamic vapor sorption analyzer (TA Instruments, New Castle, DE) equipped with a humidity controlled chamber and an ultrasensitive thermobalance. Approximately 15 to 25 mg of sample was placed into the sample pan and dried at 37°C and 0 % humidity until the weight change was less than 0.01 wt% over 5 min. Subsequently, the moisture sorption isotherm was measured by equilibrating the sample under controlled relative humidity (RH) ranging from 5 % RH to 95 % RH, in 10 % RH intervals. Equilibrium was assumed to be attained when the weight change was less than 0.01 wt% over 5 min at each RH step. Moisture sorption isotherms were obtained on three individually prepared samples of each compound analyzed.

To further evaluate the crystallization behavior of the different compounds, powder X-Ray Diffraction (PXRD) was used. To obtain sufficient material for measurements, experiments were scaled up based on the original titrations. Samples were prepared as follows: Briefly, the drugs were added to jars (16 OZ. Qorpak, Bridgeville, PA, USA; 2 bottles were used in the case of carvedilol) containing the specified volumes of demineralized water (NANOpure II, Barnstead International, Dubuque, IA, USA) and 0.5 N HCl solution, and were equilibrated at 37°C using a shaking incubator (Dubnoff Metabolic Shaking Incubator, Precision Scientific Co., Chicago, IL). Where necessary, dissolution of the drugs was aided by manually shaking the jars and/or ultrasonification (Model 8892 Ultrasonic Cleaner, Cole-Parmer, Vernon Hills, IL). In the case of bifonazole, an amorphous film, prepared by quench cooling, was used, as dissolution of the crystalline material was extremely slow. After complete dissolution of the drugs, precipitation was induced by rapidly adding 0.5 N KOH solution (volumes used are specified in Table II). Subsequently, the precipitates formed were isolated by one of three collection methods. For precipitates that tended to float (clozapine), the material was collected with a spatula. For compounds that tended to form large agglomerates in suspension (bifonazole, dipyridamole and pyrimethamine), precipitate was collected by filtering through tissue paper (11 cm×21 cm Delicate Task Wipers, Kimberly-Clark, Dallas, TX). For compounds that could not be isolated with a spatula or by filtration (carvedilol, clotrimazole, droperidol, ketoconazole, loratadine and papaverine), material was isolated by centrifugation in 50 ml tubes (BD Falcon, BD, Franklin Lakes, NJ) using an Allegra® X-15R centrifuge equipped with a SX4750 rotor (Beckman Coulter, Inc., Brea, CA). The conditions for centrifugation were 4000 RPM, 15 min, and 37°C. Samples were loaded onto aluminum sample holders and the water content of the samples was further minimized by carefully blotting with tissue paper (11 cm×21 cm Delicate Task Wipers, Kimberly-Clark, Dallas, TX, USA). PXRD analysis was performed using a Shimadzu XRD-6000 (Shimadzu Scientific Instruments, Columbia, MD, USA) equipped with a Cu-K_α source and set in Bragg-Brentano geometry. The scan range was set between 5 and 35 °2θ, and the scan speed was set to 4 °/min with a 0.02 ° step size.

Table I Summary of Compound and Precipitate Properties. Glass Transition Temperature (T_g) of the Precipitate was Noted if a Glass Transition Event was Observed

Compound	pKa(s)	Solution Behavior	Birefringence	Melting point (°C)	Precipitate T_g (°C)	PXRD	Crystallization Tendency Classification (melt quench) (13)	Crystallization Tendency Classification (solvent evaporation) (14)
Bifonazole	6.22	Type 1	Yes	149	-	Crystalline	II	II
Carvedilol	7.75	Type 2	No	117	38	Amorphous	III	III
Clotrimazole	5.89	Type 2	No	145	28	Amorphous	III	III
Clozapine	3.83, 7.54	Type 2	No	185	56	Amorphous	III	III
Dipyridamole	<1, 6.08	Type 1	Yes	164	-	Crystalline	I	III
Droperidol	<2, 7.38, 10.96	Type 1	Yes	143	-	Crystalline	II	III
Ketoconazole	3.16, 6.13	Type 2	No	149	45	Amorphous	III	III
Loratadine	5.26	Type 2	No	136	29	Amorphous	III	II/III
Papaverine	6.29	Type 1	Yes	148	-	Crystalline	III	II
Pyrimethamine	7.07	Type 1	Yes	242	-	Crystalline	N/A	N/A

Before measurements, the accuracy of the 2θ angle was checked by verifying that the [1 1 1] peak of a Si-standard sample was located between 28.423 and 28.463 °2θ. In all of the cases, measurements were initiated within an hour of inducing precipitation. In cases where no centrifugation was needed for isolation, measurements were initiated within 30 min.

Solubility and Concentration Determination

For equilibrium solubility measurements, an excess of the compound of interest was equilibrated by stirring in a buffer solution whereby the pH was at least two units above the compound pKa, at 37°C for 72 h. The solution was separated from the remaining solid phase by ultracentrifugation as described above. The supernatant was also obtained from samples containing precipitated materials, generated by pH titration (with the Sirius GLpKa instrument) to a pH at least two units above pKa of the compound, followed by ultracentrifugation. The solution concentrations were determined using an Agilent 1100 high performance liquid chromatography (HPLC) system (Agilent Technologies, Santa Clara, CA) with a 4.6×100 mm SymmetryShield RP8 3.5 μ column (Waters Chromatography, Milford, MA). An isocratic method with a flow rate of 1 ml/min was used and the mobile phase consisted of mixtures of acetonitrile and pH 2.5 phosphate buffer with the ratio adjusted to optimize the retention time to no greater than 5 min for each compound. The percentage of acetonitrile in the mobile phase was 40 % for bifonazole, carvedilol and loratadine, 35 % for clotrimazole, 30 % for ketoconazole and dipyridamole, 25 % for papaverine and pyrimethamine, and 20 % for clozapine. UV detection was employed and detection wavelengths were 230 nm for clotrimazole, 244 nm for ketoconazole, 248 nm for loratadine, 251 nm for papaverine, 253 nm for bifonazole, 272 nm for pyrimethamine, 280 nm for carvedilol, 284 nm for dipyridamole and 288 nm for clozapine. Samples for injection were adjusted by addition of acetonitrile to the same organic/aqueous ratio as the composition of the corresponding mobile phase. Samples with a concentration exceeding the linear

Table II Summary of pH-Induced Precipitate Sample Preparation for PXRD

Compound	Scale Up Factor	Drug (mg)	Water (ml)	0.5 N HCl (ml)	0.5 N KOH (ml)
Bifonazole	25	312.5	375	11.1	11.5
Carvedilol	40	301.6	600	1.86	2.18
Clotrimazole	20	304.0	300	9.4	9.5
Clozapine	6	343.3	60	5.7	5.7
Dipyridamole	20	309.8	300	11.0	11.1
Droperidol	25	346.8	375	13.2	13.5
Ketoconazole	15	404.7	150	11.6	11.8
Loratadine	20	328.2	200	6.8	6.8
Papaverine	20	313.0	300	10.7	11.0
Pyrimethamine	20	335.2	300	11.7	11.0

range were diluted accordingly and the injection volume was 20 µl. Linear ranges encompassing the sample concentrations and correlation coefficients (R^2 values) of no less than 0.999 were obtained.

Absorption Modeling

Dipryidamole and loratadine, both established marketed products, are used to illustrate the pharmaceutical relevance of type 1 and type 2 behavior respectively. For dipyramidole, GastroPlus™ modeling simulations using a compartmental absorption model were performed. Here, *in vivo* data obtained from dogs dosed with 50 mg of dipyridamole and pretreated with pentagastrin (0.006 mg/kg, IM to ensure the stomach pH was low) was used to develop and refine the model. Table III summarizes the data used to generate the model and the resultant model showed an excellent fit to the measured plasma concentrations in dog. Using this model, the influence of precipitation rate on absorption as a function of dose was simulated. For loratadine, due to the absence of available *in vivo* data, a model called microscopic mass balance approach (abbreviated to MiMBA) (20) was used to compare the predicted absorption of the drug either using the equilibrium crystal solubility, or the supersaturated concentration value determined experimentally.

RESULTS

The model compounds selected for this study are all weakly basic (see Table I for pKa values) and therefore would be expected to be soluble at low pH and precipitate when the pH is increased. The solution behavior in response to changing pH was monitored using the potentiometric titration method described above, while the precipitation outcome was evaluated by analyzing the solid state properties of the precipitant. Relevant properties of the ten weakly basic compounds, as well as their precipitation behavior are summarized in Table I. For the ten compounds studied, five (bifonazole, dipyridamole, droperidol, papaverine and pyrimethamine) were found to supersaturate prior to undergoing precipitation, exhibiting the type 1 behavior discussed above, with the supersaturation decreasing rapidly with increasing pH and the compounds forming crystalline precipitates. The other five compounds (carvedilol, clotrimazole, clozapine, ketoconazole and loratadine) behaved quite differently, precipitating rapidly and producing amorphous forms for extended periods of time and responding immediately to small changes in pH, and this is termed type 2 behavior. It should be noted that the amorphous precipitate from type 2 behavior compounds also gives rise to supersaturation and a corresponding solubility advantage, but this is different from that observed for type 1 compounds, and this will be described in more detail in the following sections.

Table III GastroPlus Parameter Summary for Dipyridamole

Simulation software	GastroPlus version 7.0.0017
	Asf Model: User defined
	Physiology: Beagle - fasted
Permeability	1.5 cm/s $\times 10^{-4}$ (21)
pKa	0.8, 6.08
Reference solubility	0.005 mg/mL pH 8.62
Solubility at low pH 1	26 mg (21)
Dog *in-vivo* data (Dog_110004_arm_2)	Oral: Pretreatment with pentagastrin (0.006 mg/kg, IM) followed by capsule containing dipyridamole in a suspension (5 mg/Kg=50 mg dose)
	IV: 1 mg/Kg

Type 1 Solution Behavior

Figure 2a shows a plot of the neutral species concentration as a function of time for dipyramidole, illustrating the pattern of behavior exhibited by type 1 compounds. During the titration, the pH increases and the neutral species concentration increases. At a certain concentration, precipitation occurs and the neutral species concentration in solution is reduced as the neutral form precipitates. Thus the supersaturation generated by increasing the pH is relatively short-lived; in this case lasting about 15 min. The peak concentration reached is 71.3 µg/ml, leading to a maximum supersaturation of 12.5 (where supersaturation is defined as the ratio of peak concentration and equilibrium solubility determined by using pH-metric titration). The supersaturation factor is 4.6, whereby the supersaturation factor was defined by Bevernage *et al.* (22) as the ratio of the total area under the solution-time concentration profile to the area under the equilibrium solubility curve (see Fig. 2b, Area A+B/Area A). For other type 1 compounds, similar behavior was observed in terms of generation of a relatively short-lived supersaturation event, although the extent and duration of the supersaturation varied between the various compounds. Results are summarized in Table IV.

An alternative way of examining the data is through means of a Bjerrum plot, which is shown in Fig. 2c for dipyridamole. A Bjerrum plot shows the relationship between hydrogen-ion binding capacity and pH. Since the model compound was a base, the titration was carried out from low to high pH, hence the number of bound protons is higher at the start of the experiment when the ionized form is present and decreases as protons are released. If all compound remains in solution, the curve is given by Eq. 1:

$$Bj = \frac{[H^+]}{[H^+] + K_a} \quad (1)$$

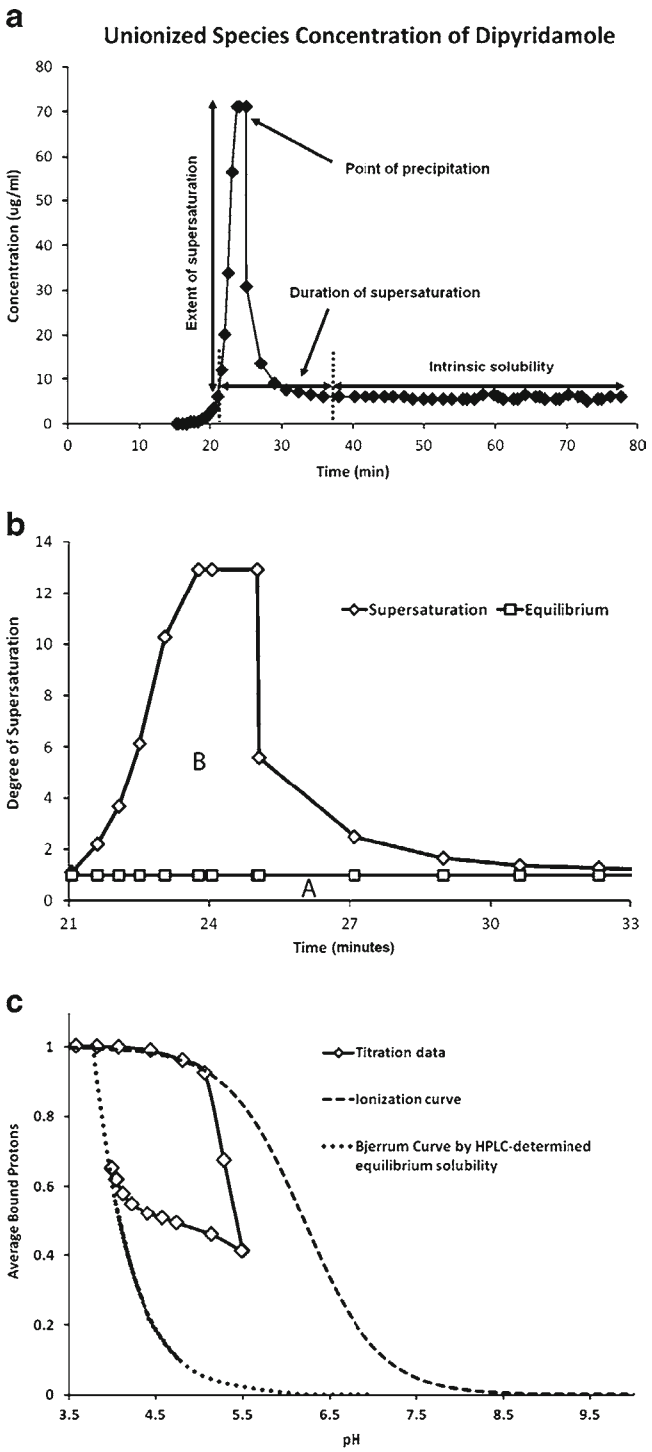

Fig. 2 (**a**) Dipyridamole unionized form concentration as function of time; (**b**) Degree of supersaturation for dipyridamole; (**c**) Bjerrum plot of dipyridamole. Dipyridamole followed the non-precipitation (aqueous pKa) theoretical curve prior to precipitation. The titration data deviated from the non-precipitation curve due to precipitation. During the chasing equilibrium process, the titration data retreated further left to lower pH and finally reached the theoretically determined Bjerrum curve using Eq. 2.

where $[H^+]$ is the total concentration of H^+ ions (calculated from the pH measurement) and K_a is the ionization constant.

During the initial titration period, when the pH is still quite low, the titration data follows the non-precipitation theoretical curve calculated from Eq. 1, which in essence is simply the theoretical ionization curve generated using the compound pK_a and this curve would be seen if no precipitation occurs (24). As pH increases, the solute precipitated and the titration data deviated from the non-precipitation theoretical curve. In the presence of a second phase, the Bjerrum curve is given by Eq. 2 (12):

$$Bj = \frac{S_0[H^+]}{X_{Total}\ K_a} \tag{2}$$

where the S_0 is the solubility of the second phase (in the case of a crystalline precipitate, the intrinsic solubility) and $[X_{total}]$ is the total concentration of sample. It can be seen that immediately following precipitation, the data lies in between the two curves, but subsequently moves towards the predicted curve for a precipitated system which was generated using the intrinsic solubility of the crystalline substance and Eq. 2. This result is consistent with the precipitate having the same solubility as the intrinsic free base solubility.

The point of precipitation was detected by UV/Vis spectroscopy from the increase in turbidity, and triggered an experimental sequence of monitoring pH and adding acidic and basic titrants to vary the solution concentration between subsaturation and supersaturation with addition of acid and base respectively. After addition of the acid or base titrant, the system moves towards equilibrium, either by dissolution of a small amount of the precipitate or further precipitation, and a pH gradient is generated with respect to time due to the consumption or release of protons by dissolving or precipitating solid when the system is near equilibrium. An example of the change in pH as a function of time following addition of an aliquot of base is shown in Fig. 3a. The starting pH prior to addition of base was 4.14 for dipyridamole. Upon addition of the base, the pH increases instantaneously. The increase in pH leads to precipitation of dipyrimadole, which releases protons and leads to a subsequent decrease in pH. This decrease is still evident after 150 s as shown by Fig. 3a. The pH gradient was obtained by calculating the rate of pH change during chasing equilibrium. The pH gradient with respect to time can be calculated and plotted following addition of acid or base. A zero pH gradient is obtained when oscillating between the positive and negative pH gradients and the concentration of the neutral species at the zero pH gradient point represents the equilibrium solubility of the precipitate since there is no net dissolution or precipitation at this point. A plot of the pH gradients obtained following addition of small aliquots of acid or base is shown in Fig. 3b for an entire chasing equilibrium experiment. The neutral species concentration

Table IV Summary of Type 1 Compound Solubility Data

Compounds (Type 1)	Equilibrium solubility[a] (HPLC)	Equilibrium solubility[a] (pH titration)	Kinetic Solubility[a] (pH titration)	Degree of supersaturation[b]	Supersaturation Duration (min)	Supersaturation factor (22)
Bifonazole	<1[c]	0.3	0.8	2.8	4.3	3.0
Dipyridamole	4.0 ± 0.5	5.7	71.3	12.5	14.7	4.6
Droperidol	4.1 (30°C) (23)[d]	3.1	82.0	26.7	6.4	12.9
Papaverine	20.6 ± 0.5	17.2	56.2	3.3	9.2	4.8
Pyrimethamine	25.0 ± 0.4	25.4	34.7	1.4	3.1	2.8

[a] Solubility unit is μg/ml

[b] Based on solubility values obtained from pH titration

[c] Out of linearity range

[d] Literature value of droperidol equilibrium solubility was reported here due to significant degradation after stirring in 37°C for 72 hours in this study

at each of the crossing points can be calculated from the experimental parameters and is in good agreement with crystalline solubility values reported in the literature or determined in this study for all the type 1 compounds studied, as summarized in Table IV.

Type 2 Solution Behavior

The corresponding neutral species *versus* time plot for loratadine, which typifies type 2 behavior, is shown in Fig. 4a. Here it can be seen that concentration remains relatively constant following the turbidometric detection of precipitation and is maintained for the duration of the experiment. The peak concentration observed is 10.7 μg/ml whereas the solubility of the original crystalline material determined using HPLC is 1.6 μg/ml. For the other compounds, similar patterns were observed although the maximum solution concentration varied widely for the different compounds, as summarized in Table V. However, the important feature of these compounds is that whatever concentration was achieved following the increase in pH was maintained for extended periods of time.

A Bjerrum plot for the titration experiment with loratadine is shown in Fig. 4b. Following precipitation, the titration data does not follow the theoretical curve that would be predicted using Eq. 2 and an S_0 value corresponding to the solubility of the crystalline base (1.6 μg/ml, Table V, determined by using HPLC). Instead, the experimental data can be modeled using the much higher solubility value of 11.3 μg/ml which was determined from HPLC measurement of the supernatant concentration. In other words, the number of bound protons is consistently higher than would be expected based on the equilibrium solubility of the crystalline base, inferring that there is more material in solution than would be expected based on the equilibrium solubility.

The other remarkable feature of the loratadine data is that the system immediately follows the new Bjerrum relationship

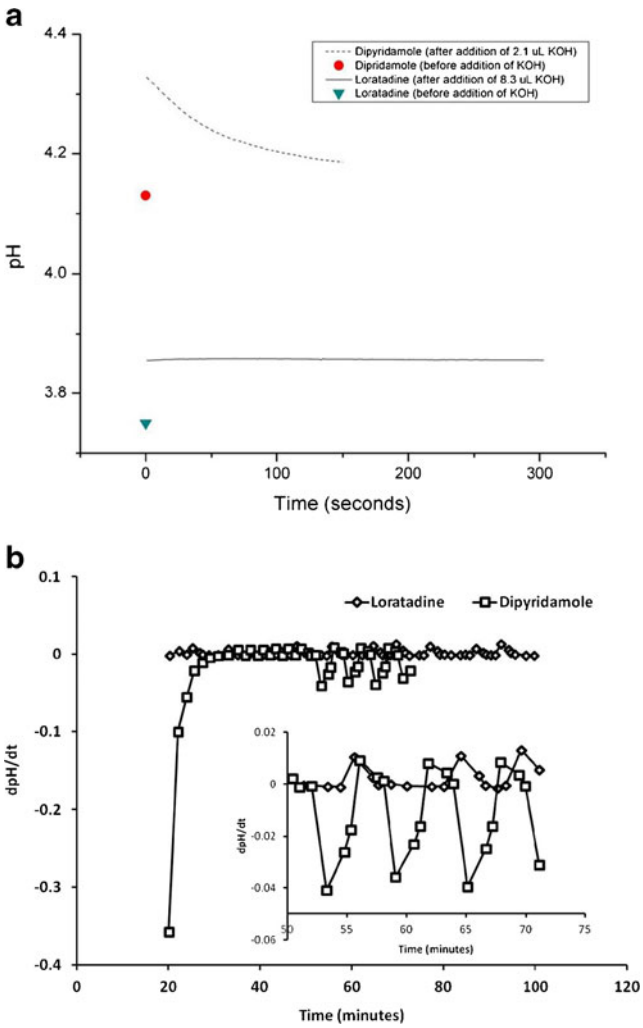

Fig. 3 (**a**) pH change upon addition of basic aliquots for dipyridamole (type 1 compound) and loratadine (type 2 compound). Following addition of KOH to dipyridamole at near equilibrium conditions the pH initially increases but subsequently shows a gradual decrease as free base drug precipitation is induced and slowly releases protons into solution. In the case of loratadine, drug precipitation occurs immediately and the system rapidly reaches a stable pH; (**b**) pH gradient of loratadine and dipyridamole during chasing equilibrium experiment.

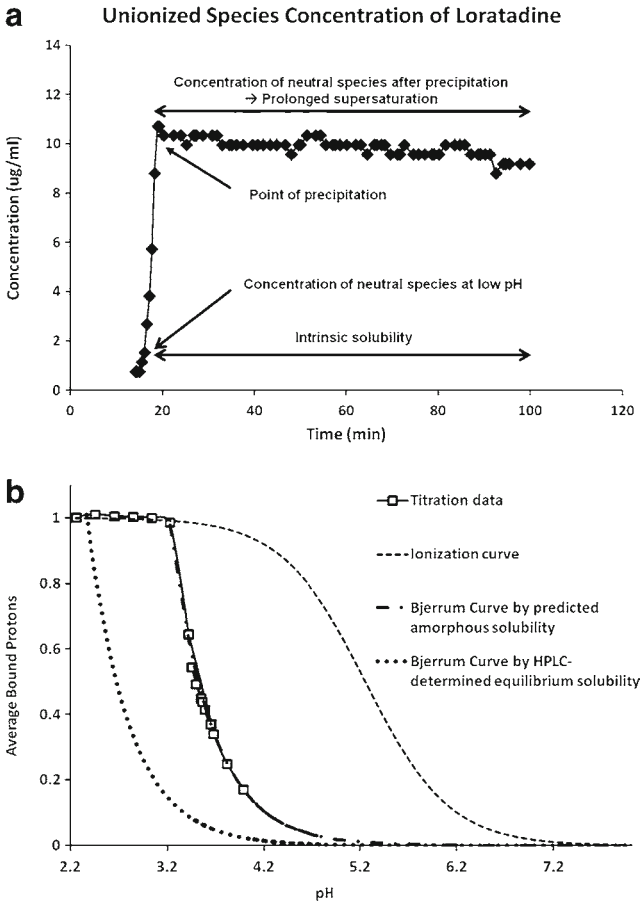

Fig. 4 (**a**) Loratadine unionized species concentration as function of time; (**b**) Loratadine titration data. Loratadine titration data deviated from the non-precipitation theoretical curve and immediately followed a precipitation theoretical curve that could be modeled using the supernatant concentration value determined by HPLC (11.3 μg/ml) which is very similar to the predicted amorphous solubility value (11.0 μg/mL). The theoretical solubility curve for the original crystalline solid is obtained from Eq. 2 using the intrinsic solubility of loratadine determined by HPLC (1.6 μg/mL).

(modeled by Eq. 2 and an S_0 value of 11.3 μg/ml) without any transition period, in contrast to that observed for dipyramidole and the other type 1 compounds. The response of the system to pH change can be further evaluated by examining a plot of pH *versus* time following addition of base, as shown in Fig. 3a. Here, the initial pH was 3.75 and following addition of base, the pH increases. However, in contrast to dipyramidole, the pH remains constant, leading to the conclusion that the system has immediately readjusted to the change in pH, in other words, the precipitation is instantaneous, suggesting a very different precipitation mechanism than for type 1 compounds. Hence, when small amounts of acid and base were added to the system containing precipitate, a minimal pH gradient with time was observed (Fig. 3b), indicating that the system immediately readjusted to the change in pH, *i.e.* the dissolution and precipitation process was much faster than for the dipyramidole case described above.

Solid State Characterization of Precipitates

Type 1 and type 2 compounds, exemplified by dipyridamole and loratadine respectively, appeared to precipitate very differently in the pH titration experiments, hence it was of interest to characterize the solid state properties of the precipitates resulting from the titration experiments. The microscopic image of dipyridamole (Fig. 5a) showed birefringent particles which were needle shaped, demonstrating that the precipitate was crystalline. The DSC thermograms showed a defined endotherm at the same temperature with a similar heat of fusion to the crystalline reference material, whereby results were also consistent with literature reported values (25) (Fig. 5b). PXRD results (Fig. 5e) confirmed that the precipitate was crystalline, with some diffuse scattering likely caused by the presence of water in the precipitate. The loratadine precipitate did not show birefringence under polarized light and the particles were of poorly defined morphology (Fig. 5c). The DSC thermogram of the loratadine precipitate (Fig. 5d) supported the disordered nature of

Table V Equilibrium Solubility and Supernatant Concentration Data for Compounds That Have Prolonged Supersaturation (Type 2 Compounds)

Compounds (Type 2)	Equilibrium solubility[a] (HPLC)	Experimental supernatant concentration[a] (HPLC)	Degree of supersaturation[b]	Predicted amorphous solubility[a,c]	Predicted amor phous solubility w/moisture sorption effect[a,c]	Equilibrium solubility[a] (pH titration)	Kinetic solubility[a] (pH titration)
Carvedilol	1.1 ± 0.1	8.68 ± 0.2	8.3	24.4 ± 2.2 (22.2)	13.53 ± 1.2 (12.3)	19.4	21.8
Clotrimazole	0.4 ± 0.02	5.09 ± 0.01	12.5	5.0 ± 0.2 (11.9)	4.00 ± 0.2 (9.8)	5.7	6.8
Clozapine	8.8 ± 0.1	157 ± 11.7	17.9	179.5 ± 2.0 (20.4)	147 ± 1.8 (16.7)	170	180
Ketoconazole	3.7 ± 0.1	76.5 ± 3.8	20.7	202 ± 5.5 (54.6)	56.6 ± 1.5 (15.3)	84.9	91.7
Loratadine	1.6 ± 0.1	11.3 ± 0.04	7.2	11.0 ± 0.7(7.0)	6.8 ± 0.4 (4.3)	9.9	10.7

[a] The unit for solubility and concentration is μg/ml

[b] Based on solubility and supernatant concentration measured by HPLC

[c] Values in the brackets are amorphous/crystalline solubility ratio

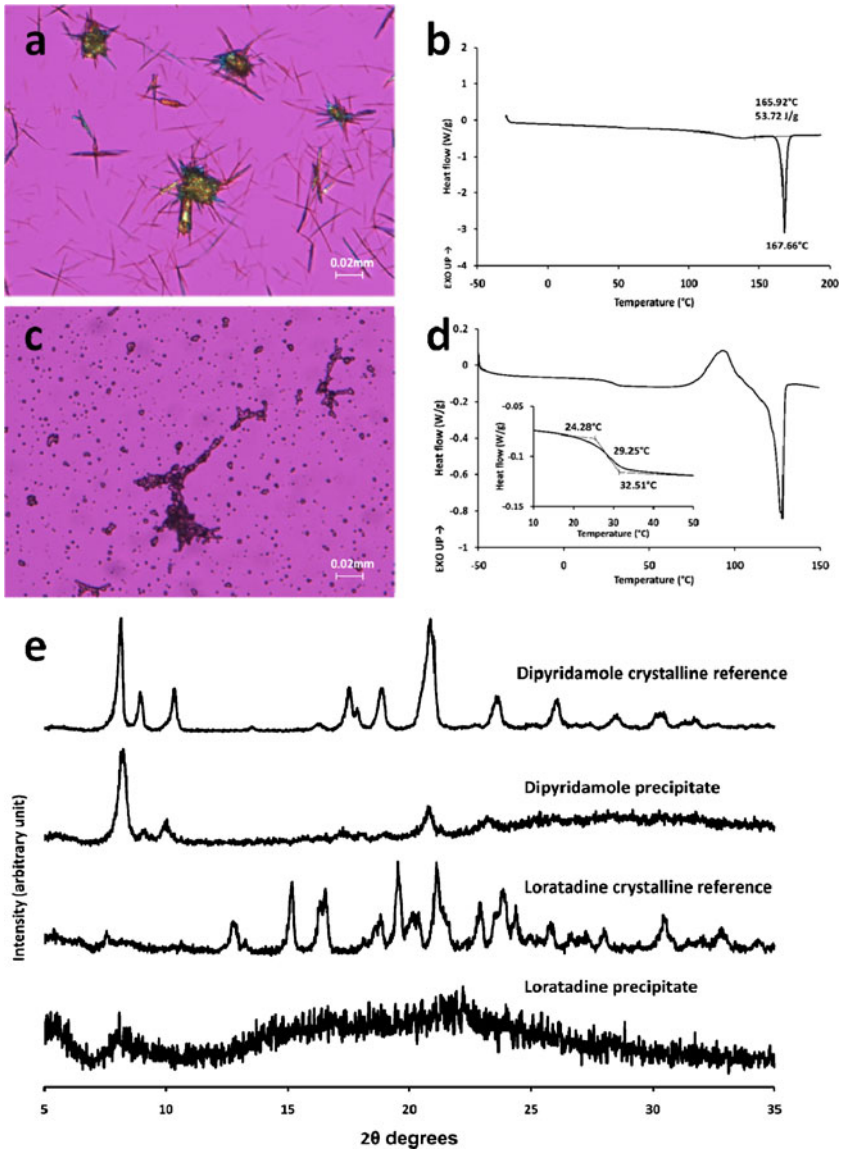

Fig. 5 (**a**) Polarized light microscope image of dipyridamole precipitate; (**b**) DSC result of dipyridamole precipitate with heating rate of 5°C/min; (**c**) Polarized light microscope image of loratadine precipitate; (**d**) DSC result of loratadine precipitate at a heating rate of 5°C/min; (**e**) PXRD results for dipyridamole and loratadine.

the precipitate suggested by the microscopic examination, with a glass transition (T_g) like event from 24°C to 32°C followed by an exothermic event (consistent with crystallization) and an endotherm at the same temperature as the reference crystalline material. The recrystallization of the sample during the heating run most likely resulted from a small amount of nucleation that occurred during sample drying, or the presence of some residual moisture. The T_g of dry loratadine has been reported previously as 37°C (13). The PXRD analysis (Fig. 5e) was also consistent with a disordered precipitate since no diffraction peaks were observed. Thus the microscopy, PXRD and calorimetry confirm the amorphous nature of the loratadine precipitate. The pH-induced precipitates of the remaining compounds were analyzed in a similar manner and results are summarized in Table I. Compounds showing type 1 behavior had crystalline precipitates, while compounds showing type 2 behavior had amorphous precipitates.

Solubility Measurements

The kinetic and equilibrium solubilities were determined from the titration data using a series of mass and charge balance equations and the chasing equilibrium method described previously. The various solubility measurements and estimates are summarized in Tables IV and V.

As the results from the solid state analyses indicate that the type 2 compounds precipitate as non-crystalline forms, it is of interest to compare the supernatant concentration after precipitation with the estimated amorphous solubility. The supernatant concentration was obtained from samples prepared by titrating the pH to two units above the pKa. The

amorphous solubility was approximated by estimating the free energy difference between crystalline and amorphous forms using the Hoffman equation (26):

$$\Delta G_c = \Delta H_f \times \frac{(T_m - T)T}{T_m^2} \tag{3}$$

The ratio of amorphous and crystalline solubility ($S_{amorphous}/S_{crystalline}$) was then estimated (using Eq. 4) from the free energy difference (ΔG_c) calculated from heat of fusion (ΔH_f) and melting temperature (T_m) of the crystalline material determined from DSC analysis, as well as the experimentally determined crystalline solubility:

$$\frac{S_{amorphous}}{S_{crystalline}} \approx \frac{a_{amorphous}}{a_{crystalline}} = \exp\left[\frac{\Delta G_c}{RT}\right] \tag{4}$$

In addition, the quantitative approach developed by Murdande *et al.* (27,28) was used to determine the impact of water in the amorphous solid on the thermodynamic activity and hence estimated solubility advantage. This method involves determining the number of moles of water absorbed per mole of solute as a function relative humidity and estimating the water content at a relative humidity of 100 (water activity of 1). The activity of the amorphous solute is estimated by applying the Gibbs-Duhem equation to water sorption isotherm data for the amorphous solid. The detailed thermodynamic analysis is presented in reference (27). The final form of the Gibbs-Duhem equation, $I(a_2)$, may be written as Eq. 5:

$$I(a_2) = \left(\frac{n_1}{n_2}\right)_{Henry} + \int_{\bar{a}_1^H}^{\bar{a}_1^S} \left(\frac{n_1}{n_2}\right)\frac{1}{a_1}da_1 \tag{5}$$

where n_1 and n_2 are moles of water and solute, respectively, $\bar{a}_1^H$ is the activity of water at the Henry's law limit and $\bar{a}_1^S$ is the activity of water in the solid in equilibrium with dilute solution ($\bar{a}_1^S$ is the extrapolated water activity at unit water activity). Equation 5 can be divided into two parts, the Henry's law region, which ranges from zero water content to the limit of linearity of water activity and a "high water" region. The first term, $\left(\frac{n_1}{n_2}\right)_{Henry}$, is the concentration value at the limit, while the integral in the "high water" region may be evaluated numerically (by the summation of the products, $\left\langle\left(\frac{n_1}{n_2}\right)\frac{1}{a_1}\right\rangle_{i+1,i}\left(a_1^{i+1} - a_1^i\right)$) using the water sorption isotherm data (27). Equation 6 represents the incorporation of water sorption effects into the thermodynamic prediction of solubility.

$$\frac{S_{amorphous}}{S_{crystalline}} = \exp[-I(a_2)] \cdot \exp\left[\frac{\Delta G_c}{RT}\right] \tag{6}$$

The predicted amorphous solubility values at 37°C with and without moisture sorption correction for type 2 compounds are summarized in Table V.

DISCUSSION

Poor oral bioavailability is recognized as a growing issue in the drug development process and this has been identified as the potential root cause of multiple issues such as low exposure or unacceptable variability or a combination of the two. The reason why this is an issue is because it increases the risk of failure during development where the efficacious dose and margins of safety needs to be defined for a new drug entity and the pharmacokinetics of a new drug entity are not known. Essentially, a range of doses to achieve different systemic exposures need to be explored during development and the inability to do this will either lead to delays arising from either reformulation of a product or increasing the clinical study size to achieve statistical significance or termination of the project.

Variable solubility within the GI tract can lead to both low and/or highly variable exposure hence the precipitation behavior of supersaturating dosage forms is an area of great current interest. However, the relationship between the phase behavior of the precipitated material and the resultant solution concentration-time profiles has not been extensively considered. Indeed, the word precipitate is a rather generic term implying only the presence of a second phase detectable with methods such as turbidimetry, and conveys no information about the structure of this second phase, such as if it is a crystalline or disordered phase. The structure of the precipitated phase is of key importance since it should theoretically impact the solution concentration-time profiles. Herein, it has been observed that precipitation outcomes can be divided into two types of phenomenological behavior: type 1 compounds whereby the precipitated material is crystalline, and type 2 compounds where the precipitate is amorphous and present for the duration of the experiment. The solution concentration time profiles are quite different between the two groups of compounds and the underlying basis for this is discussed below.

Crystallization is perhaps the expected outcome for weak bases dissolved at low pH and then subjected to an increase in pH such that the neutral species concentration exceeds the intrinsic solubility. Crystallization from solution is known to consist of two processes, nucleation of the new phase followed by growth. In order for crystal nucleation to occur, a certain extent of supersaturation must be generated, in other words the neutral species concentration must exceed the intrinsic solubility by a given amount. This is because there is an energy barrier to nucleation which arises from the unfavorable process of forming new surface. Classical nucleation theory illustrates the relationship between

the nucleation rate, J, and the supersaturation (S) as shown by Eqs. 7 and 8:

$$J \propto \exp\left(-\frac{\Delta G^*}{k_B T}\right) \tag{7}$$

$$\Delta G^* \propto \frac{1}{(\ln S)^2} \tag{8}$$

where ΔG^* is the free energy change for the formation of the new phase, k_B is Boltzmann's constant, and T is temperature. At low supersaturations, either no nucleation occurs or the nucleation rate is long relative to the experimental timeframe. As the supersaturation increases, nucleation becomes more probable and once a certain supersaturation is reached, spontaneous nucleation is observed. The critical level of supersaturation at which precipitation is seen is highly dependent not only on the compound under study, but also on the experimental conditions and hence is somewhat variable. Once nucleation has occurred and nuclei larger than the critical size have been produced, crystal growth can occur until the supersaturation is depleted, *i.e.* the solution concentration reaches the solubility value of the crystalline form. This type of behavior is seen for five of the weak bases investigated in this study where precipitation was detected once a given level of supersaturation was reached (see Table IV and Fig. 2a). For these compounds, following detection of a precipitate, the neutral species solution concentration drops with time towards that of the crystalline material, *i.e.* the intrinsic solubility is approached, consistent with the presence of a crystalline precipitate. The solid state analysis confirmed the presence of a crystalline precipitate of the same phase as the starting material and there is a good correlation between the independently measured crystal solubility using HPLC and that measured during the Cheqsol experiment (Table IV). For the five compounds, the extent and duration of supersaturation varied considerably. This can be seen by comparing the supersaturation factors, whereby the latter is a method introduced by Bevernage *et al.* (22) in order to quantitatively compare the solution-time concentration profiles. Pyrimethamine has the lowest supersaturation factor of 2.8 while droperidol has the highest value at 12.9. Compounds that crystallize following a short lived duration of supersaturation are likely to show a bioavailability profile that can be predicted by considering only equilibrium values in absorption models. However, these are also the compounds where the extent of supersaturation often can be influenced by the dose and precipitation rates modified by addition of polymers and additives. In addition, type 1 compounds may show a large intra and inter-patient variation if the crystallization behavior is significantly impacted by food effects or other *in vivo* variations. These ideas are discussed in more detail below.

Dipyridamole is used to illustrate the potential pharmaceutical relevance of type 1 behavior. Dipyridamole is a platelet adhesion inhibitor commonly used to prevent postoperative thromboembolic complications and oral doses range from 75 to 100 mg four times a day for the main indication with additional studies reporting doses of 200 to 600 mg per day for other indications (29,30). Studies assessing the bioavailability of dipyridamole have demonstrated that absorption is variable and pH dependent in humans and a canine model (31,32). This is of relevance during a clinical study because volunteers and patients recruited may be elderly exhibiting achlorhydric gastric conditions or on proton pump inhibitors and thus have elevated pH conditions which result in significantly lower exposures than the rest of the clinical population. Russell *et al.* (31) showed that pretreatment of achlorhydric subjects with glutamic HCl increased the exposure of dipryidamole as predicted. Present day, *in vitro* assays and simulation models would have predicted this exposure variability risk for dipryidamole and resulted in the development of a formulation that ensured solubility irrespective of the stomach pH. The most likely formulation option would be a solid dispersion formulation or a formulation containing a microenvironmental pH modifier. If the assumption is made that these formulations ensure that the compound is in solution in the stomach, then the question remains as to whether the molecule stays in solution when it reaches the small intestine. A sensitivity analysis was conducted using the optimized GastroPlus™ dog model described previously to assess how the predicted amount absorbed is impacted with changes in dose and precipitation rate (Fig. 6a). This analysis predicts that at a 50 mg dose (clinically relevant dose), a precipitation time between 100 and 1000 s has no impact on absorption; while at a dose of 550 mg, the amount absorbed increases significantly as the time of precipitation is increased from 100 to 1000 s. Although there is no *in vivo* data to support this model, the example shows the theoretical importance of precipitation rates (in other words, the duration of supersaturation) for type 1 behavior molecules.

Alternatively, precipitation to an amorphous form can also occur, as demonstrated from solid state analysis of the precipitated material obtained in this study. It is important to better understand the mechanism of amorphous precipitation and the corresponding solution behavior during the potentiometric experiments. In the absence of crystallization, the solubility of an amorphous solid is higher (*i.e.* the solution is supersaturated) with respect to the solubility of a crystalline form. The potentiometric experiments show that the kinetics of precipitation are rapid and immediate for type 2 compounds, and that the amorphous form is stable for long periods of time, *giving the appearance that the compounds precipitate without supersaturation* (11). In other words, the compounds precipitate when the solution concentration is close to the "amorphous solubility" and a metastable-equilibrium is maintained between the solution and the amorphous precipitate. Hence, both the potentiometric method of solubility estimation, and independent analysis of the supernatant concentration of the precipitated

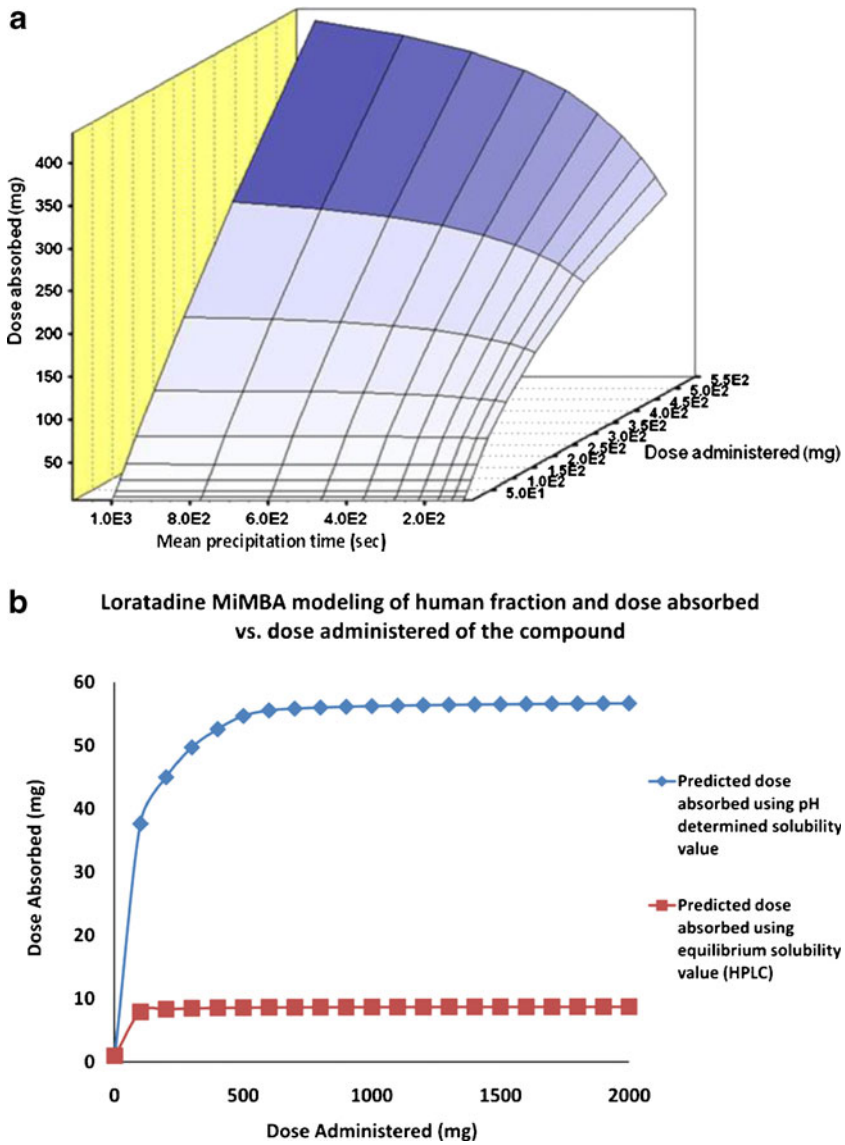

Fig. 6 (**a**) GastroPlus sensitivity analysis for the diprydamole dog simulation showing how the dose absorbed changes with mean precipitation rate and dose administered; (**b**) MiMBA prediction of dose absorbed for Loratabine using pH determined solubility values and equilibrium solubility values.

solutions (Table V), reveal that the solution concentration for these systems is elevated relative to the crystalline solubility, in other words the solution remains supersaturated with respect to the crystalline solid for a considerable period of time. Evidence that the measured solution concentration corresponds to the amorphous solubility is provided by the following observations: first it is known that the precipitated material in metastable-equilibrium with the solution is amorphous based on the PXRD, DSC and polarized light microscopy results summarized in Table I and second, the measured solution concentrations following separation from the precipitated phase corresponds well with the estimated amorphous solubility (see Eqs. 3–6 and Table V). One exception was noted: The supernatant concentration of carvedilol determined by HPLC is somewhat lower than either the theoretically predicted amorphous solubility (with or without moisture sorption correction) or the solubility values obtained by pH-metric titration, which may be attributed to conversion to a less soluble form during ultracentrifugation, possibly a liquid crystalline form given the lack of diffraction peaks seen from PXRD. The solubility values obtained by using pH-metric titration do, however, agree with theoretically predicted amorphous solubility values, suggesting that this transient state is captured in the latter experiment. It is important to point out that the potentiometric method thus provides a new avenue for the experimental determination of amorphous solubility for certain types of compounds (type 2), and could provide substantial advantages over existing methods. First, it does not require the production of a reference amorphous solid and second, no sample manipulation (such as filtering or centrifugation), which can influence the crystallization behavior of the solution, is required. This is an important finding as it is notoriously difficult to arrive at pseudo equilibrium amorphous solubility measurements experimentally due to either

crystallization of the dissolving amorphous material or crystallization from the supersaturated solution that is generated on dissolution (33).

Based on the experimental observations, as well as theoretical concepts, we believe that the behavior of the type 2 compounds showing amorphous precipitation and displaying extended supersaturation (with respect to the crystalline form) can be best explained by considering the phenomenon of liquid-liquid (L-L) phase separation, where the "liquid" undergoing phase separation from the mother solution phase can be an amorphous supercooled liquid or a glassy solid, since the process is occurring at a temperature below the melting point of the crystalline material. If the compound is above its melting point, this process is sometimes termed "oiling out". However, in all cases, a liquid-like phase (amorphous glass, supercooled liquid or equilibrium liquid) is separating out from the bulk solution phase, so the generic term liquid-liquid phase separation will be used herein.

L-L phase separation can occur at high supersaturation resulting in the formation of two liquid phases (34). This phenomenon has been reported to occur for a number of organic compounds (35–44). L-L phase separation will always occur if the compound is above its melting point, or there is no crystalline form and the L-L miscibility point is exceeded. However, L-L phase separation can also occur even if crystalline forms exist and in this case, L-L phase separation can be regarded as a metastable phase transformation that precedes crystallization whereby crystallization can subsequently occur from either of the two liquid phases. For example, Roberts *et al.* suggest that L-L phase separation is a precursor to citric acid crystallization, seen in highly supersaturated solutions (43). L-L phase separation produces two liquid phases each of a composition different from the original homogeneous solution phase. Experimental studies have shown that the metastable zone for L-L phase separation is very small; in other words, little supersaturation (with respect to the equilibrium L-L phase separation concentration) is actually observed (44,45). For the type 2 compounds, it was observed experimentally that turbidity (indicative of the presence of a second scattering phase) evolved at a concentration very close to the final concentration observed in the experiment. In other words, there was little to no supersaturation (relative to the L-L phase separation concentration), consistent with a facile phase separation process. Furthermore, Fig. 3a showed that when the pH was altered to induce small changes in the saturation state, the response of the system was instantaneous, in contrast to the crystalline systems, again consistent with a very low energy barrier for the mass transfer between the two phases (dissolution or growth of the disperse phase). Interestingly, many compounds where the free base form has a melting point lower than room temperature, and hence they exist as a liquid or "oil" at room temperature, also show Type 2 behavior. These include compounds such as amitriptyline, chlorpromazine, desipramine, fluoxetine and pramoxine (11,46). However, in the case of the compounds investigated in this study, the melting points of the free base are all well above room temperature (>110°C), therefore L-L phase separation results in a metastable system that can undergo subsequent crystallization from either phase. Despite the difference in the nature of the equilibrium phase at room temperature, the phenomenological behavior of the "oils" and the amorphous precipitates are very similar, supporting our supposition that this process can be regarded as L-L phase separation.

Weakly basic compounds that precipitate as type 2 behavior are likely to show a bioavailability that is higher than expected since they produce amorphous forms that are more soluble and reluctant to crystallize, resulting in prolonged supersaturation. This is illustrated by Fig. 6b which shows biopharmaceutical modeling of loratadine using a Eli Lilly & Company proprietary prediction absorption model based on microscopic mass balance approach (abbreviated to MiMBA). This type of modeling is often used to estimate the fraction absorbed for a given dose delivered and used during the discovery phase (commonly lead optimization stage) to simply assess where a drug sits in the "biopharmaceutical landscape" so that it can be prioritized for further progression or to determine the strategies for formulation selection. The figure shows that the maximum absorbable dose predicted for loratadine using the intrinsic solubility value (HPLC shake flask method commonly used by most laboratories) is significantly lower than that predicted used the titration determined solubility value. Moreover, the amorphous particles are likely to be rapidly dispersed during transit along the GI tract and readily absorbed on further dilution which is not taken into account in any of the absorption models currently available.

The supersaturation behavior of the type 1 and type 2 compounds appears also to be highly correlated to their inherent crystallization tendency. Previous studies have shown that compounds have very different crystallization tendencies both on cooling from the melt as well as during rapid solvent evaporation (13,14) and compounds have been classified as fast, intermediate or slow crystallizers depending on the behavior shown during solidification processes. These classifications are shown in Table I for the model compounds evaluated in this study. It is apparent that all of the compounds that exhibited type 2 behavior tend to fall into the category of slow crystallizers. The crystallization behavior of type 1 compounds was more variable and dependent on the evaluation method. It thus appears that the tendency to crystallize or not during pH induced precipitation is also linked to molecular structure and generally correlates to some extent with crystallization during other solidification processes including melt crystallization, and/

or during rapid solvent evaporation. However, the crystallization tendency upon precipitation from an aqueous environment would be expected to also depend on additional factors, in particular the presence of water which will promote molecular mobility of an amorphous phase generated. Given the longevity of the amorphous material in an unfavorable environment (*i.e.* aqueous), type 2 behavior may also correlate with the ability to form stable amorphous formulations having long shelf-life stability and yielding long-lived supersaturated solutions upon dissolution. Finally, this assignment may also be used to predict whether a compound will form a crystalline free form.

CONCLUSION

In this study, two different types of precipitation behavior were observed for weakly basic compounds from supersaturated solutions generated by pH increases. Type 1 behavior resulted in a crystalline precipitate, while type 2 behavior yielded an amorphous precipitate and a solution supersaturated with respect to the crystalline counterpart. Thus it seems apparent that highly supersaturated solutions of a crystallizing compound can either directly crystallize or undergo liquid-liquid phase separation leading to a two phase supersaturated solution from which crystallization can occur subsequently. The precipitation to a non-crystalline phase with the resultant elevated solution concentration levels has important implications for several areas of pharmaceutical development including: 1) the ability to accurately predict absorption using modeling 2) risk assessment for solid dispersion formulations and the subsequent tendency of the API to remain in solution following dissolution, 3) design of oral formulations that minimize variation, and potentially 4) formulation of parenteral systems where solubilization is required.

ACKNOWLEDGMENTS & DISCLOSURES

The authors would like to thank Eli Lilly and Company for providing the Sirius instrument. Pfizer Inc. is acknowledged for providing a fellowship for YLH. BVE is a Postdoctoral Researcher of the 'Fonds voor Wetenschappelijk Onderzoek', Flanders, Belgium.

REFERENCES

1. Li S, He H, Parthiban LJ, Yin H, Serajuddin ATM. IV-IVC considerations in the development of immediate-release oral dosage form. J Pharm Sci. 2005;94(7):1396–417.
2. Hillery AM, Lloyd AWS, J. Drug delivery and targeting: for pharmacists and pharmaceutical scientists. 1 edition ed: CRC Press; 2001.
3. Mullin JW. Crystallization. 4th edition. Oxford: Elsiever Butterworth-Heinemann; 2001.
4. Vandecruys R, Peeters J, Verreck G, Brewster ME. Use of a screening method to determine excipients which optimize the extent and stability of supersaturated drug solutions and application of this system to solid formulation design. Int J Pharm. 2007;342(1–2):168–75.
5. Gao P, Rush BD, Pfund WP, Huang T, Bauer JM, Morozowich W, *et al.* Development of a supersaturable SEDDS (S-SEDDS) formulation of paclitaxel with improved oral bioavailability. J Pharm Sci. 2003;92(12):2386–98.
6. Yang S, Gursoy RN, Lambert G, Benita S. Enhanced oral absorption of paclitaxel in a novel self-microemulsifying drug delivery system with or without concomitant use of P-Glycoprotein inhibitors. Pharm Res. 2004;21(2):261–70.
7. DiNunzio JC, Miller DA, Yang W, McGinity JW, Williams RO. Amorphous compositions using concentration enhancing polymers for improved bioavailability of itraconazole. Mol Pharm. 2008;5(6):968–80.
8. Miller DA, DiNunzio JC, Yang W, McGinity JW, Williams RO. Enhanced *in vivo* absorption of itraconazole via stabilization of supersaturation following acidic-to-neutral pH transition. Drug Dev Ind Pharm. 2008;34(8):890–902.
9. Curatolo W, Nightingale J, Herbig S. Utility of Hydroxypropylmethylcellulose Acetate Succinate (HPMCAS) for initiation and maintenance of drug supersaturation in the GI Milieu. Pharm Res. 2009;26(6):1419–31.
10. Brouwers J, Brewster ME, Augustijns P. Supersaturating drug delivery systems: the answer to solubility-limited oral bioavailability? J Pharm Sci. 2009;98(8):2549–72.
11. Box KJ, Völgyi G, Baka E, Stuart M, Takács-Novák K, Comer JEA. Equilibrium *versus* kinetic measurements of aqueous solubility, and the ability of compounds to supersaturate in solution - a validation study. J Pharm Sci. 2006;95(6):1298–307.
12. Stuart M, Box K. Chasing equilibrium: measuring the intrinsic solubility of weak acids and bases. Anal Chem. 2005;77(4):983–90.
13. Baird JA, Van Eerdenbrugh B, Taylor LS. A classification system to assess the crystallization tendency of organic molecules from undercooled melts. J Pharm Sci. 2010;99(9):3787–806.
14. Van Eerdenbrugh B, Baird JA, Taylor LS. Crystallization tendency of active pharmaceutical ingredients following rapid solvent evaporation—classification and comparison with crystallization tendency from undercooled melts. J Pharm Sci. 2010;99(9):3826–38.
15. Miyajima M, Koshika A, Okada J, Ikeda M, Nishimura K. Effect of polymer crystallinity on papaverine release from poly (l-lactic acid) matrix. J Controlled Release. 1997;49(2–3):207–15.
16. Allen RI, Box KJ, Comer JEA, Peake C, Tam KY. Multiwavelength spectrophotometric determination of acid dissociation constants of ionizable drugs. J Pharm Biomed Anal. 1998;17(4–5):699–712.
17. Avdeef A, Comer JEA, Thomson SJ. pH-Metric log P. 3. Glass electrode calibration in methanol–water, applied to pKa determination of water-insoluble substances. Anal Chem. 1993;65(1):42–9.
18. Takács-Novák K, Box KJ, Avdeef A. Potentiometric pKa determination of water-insoluble compounds: validation study in methanol/water mixtures. Int J Pharm. 1997;151(2):235–48.
19. Avdeef A. pH-metric log P. II: Refinement of partition coefficients and lonization constants of multiprotic substances. J Pharm Sci. 1993;82(2):183–90.
20. Oh D-M, Curl RL, Amidon GL. Estimating the fraction dose absorbed from suspensions of poorly soluble compounds in humans: a mathematical model. Pharm Res. 1993;10(2):264–70.
21. Kostewicz ES, Brauns U, Becker R, Dressman JB. Forecasting the oral absorption behavior of poorly soluble weak bases using solubility and dissolution studies in biorelevant media. Pharm Res. 2002;19(3):345–9.

22. Bevernage J, Forier T, Brouwers J, Tack J, Annaert P, Augustijns P. Excipient-mediated supersaturation stabilization in human intestinal fluids. Mol Pharm. 2010;8(2):564–70.
23. Yalkowsky SH, He Y. Handbook of aqueous solubility data. 1 edition. CRC Press; 2003.
24. Avdeef A. pH-metric solubility. 1. Solubility-pH profiles from Bjerrum plots. Gibbs buffer and pKa in the solid state. Pharm Pharmacol Commun. 1998;4:165–78.
25. Berbenni V, Marini A, Bruni G, Maggioni A, Cogliati P. Thermoanalytical and spectroscopic characterization of solid state dipyridamole. J Therm Anal Calorim. 2002;68(2):413–22.
26. Hoffman JD. Thermodynamic driving force in nucleation and growth processes. J Chem Phys. 1958;29(5):1192–3.
27. Murdande SB, Pikal MJ, Shanker RM, Bogner RH. Solubility advantage of amorphous pharmaceuticals: I. A thermodynamic analysis. J Pharm Sci. 2009;99(3):1254–64.
28. Murdande S, Pikal M, Shanker R, Bogner R. Solubility advantage of amorphous pharmaceuticals: II. Application of quantitative thermodynamic relationships for prediction of solubility enhancement in structurally diverse insoluble pharmaceuticals. Pharm Res. 2010;27(12):2704–14.
29. DRUGDEX® System [Internet database]. Greenwood Village, Colo: Thomson Reuters (Healthcare) Inc. Updated periodically.
30. Micromedex® Healthcare Series [Internet database]. Greenwood Village, Colo: THOMSON REUTERS (Healthcare) Inc. Updated periodically.
31. Russell TL, Berardi RR, Barnett JL, O'Sullivan TL, Wagner JG, Dressman JB. pH-related changes in the absorption of dipyridamole in the elderly. Pharm Res. 1994;11(1):136–43.
32. Zhou R, Moench P, Heran C, Lu X, Mathias N, Faria TN, *et al.* pH-dependent dissolution *in vitro* and absorption *in vivo* of weakly basic drugs: development of a canine model. Pharm Res. 2005;22(2):188–92.
33. Alonzo D, Zhang G, Zhou D, Gao Y, Taylor L. Understanding the behavior of amorphous pharmaceutical systems during dissolution. Pharm Res. 2010;27(4):608–18.
34. Tung H-H, Paul EL, Midler M, McCauley JA. Critical issues in crystallization practice. Crystallization of Organic Compounds: John Wiley & Sons, Inc.; 2008. p. 101–16.
35. Bonnett PE, Carpenter KJ, Dawson S, Davey RJ. Solution crystallisation via a submerged liquid-liquid phase boundary: oiling out. Chem Commun. 2003;6:698–9.
36. Veesler S, Lafferrère L, Garcia E, Hoff C. Phase transitions in supersaturated drug solution. Org Process Res Dev. 2003;7(6):983–9.
37. Codan L, Bäbler MU, Mazzotti M. Phase diagram of a chiral substance exhibiting oiling out in cyclohexane. Cryst Growth Des. 2010;10(9):4005–13.
38. Derdour L. A method to crystallize substances that oil out. Chem Eng Res Des. 2010;88(9):1174–81.
39. Svärd M, Gracin S, Rasmuson ÅC. Oiling out or molten hydrate—liquid–liquid phase separation in the system vanillin–water. J Pharm Sci. 2007;96(9):2390–8.
40. He G, Tan RBH, Kenis PJA, Zukoski CF. Metastable States of Small-Molecule Solutions. J Phys Chem B. 2007;111(51):14121–9.
41. Roelands CPM, ter Horst JH, Kramer HJM, Jansens PJ. Precipitation mechanism of stable and metastable polymorphs of L-glutamic acid. AICHE J. 2007;53(2):354–62.
42. Lafferrère L, Hoff C, Veesler S. Study of liquid-liquid demixing from drug solution. J Cryst Growth. 2004;269(2–4):550–7.
43. Groen H, Roberts KJ. Nucleation, growth, and pseudo-polymorphic behavior of citric acid as monitored *in situ* by attenuated total reflection fourier transform infrared spectroscopy. J Phys Chem B. 2001;105(43):10723–30.
44. Maeda K, Aoyama Y, Fukui K, Hirota S. Novel phenomena of crystallization and emulsification of hydrophobic solute in aqueous solution. J Colloid Interface Sci. 2001;234(1):217–22.
45. Lai SM, Yuen MY, Siu LKS, Ng KM, Wibowo C. Experimental determination of solid–liquid-liquid equilibrium phase diagrams. AICHE J. 2007;53(6):1608–19.
46. Box KJ, Comer JEA. Using measured pK(a), LogP and solubility to investigate supersaturation and predict BCS class. Curr Drug Metab. 2008;9(9):869–78.